Chemical Process Design Vol.5 No.1 (2026) 54-61

University of Sistan and Baluchestan

Chemical Process Design

Available online at http://cpd.usb.ac.ir/

University of Sistan and Baluchestan
CPD CHEMICAL PROCESS DESIGN
Editor-in-Chief
Prof. Farhad Shahraki
Editor in Charge
Dr. Mohammadreza Sardashti Birjandi
Executive Manager
Dr. Bahareh Bidar
Volume 5, Issue 1
June 2026
ISSN 2980-8707
FEATURED ARTICLE

Determining Thermodynamic Conditions for Petroleum Wax Formation using Activity Models in Solid-Liquid and Solid-Gas Equilibria

Zahra Ghafourian[1], Mohammad Fani Kheshti[2,3], Mojtaba Saei Moghaddam[1]✉

[1]Chemical Engineering Department, Faculty of Advanced Technologies, Quchan University of Technology, Quchan, Iran.
E-mail: zgh2650@gmail.com
[2]Center of Maghsoud Porcelain Complex, National, University of Applied Science and Technology, Tehran, Iran.
E-mail: fany62m@yahoo.com
[3]Corresponding Author, Department of Chemical Engineering, Faculty of Engineering, Ferdowsi University of Mashhad, Mashhad, Iran.
E-mail: mojtabasaei@qiet.ac.ir

ARTICLE INFO

Article type:
Research Article

Article history:
Received: 2025-08-13
Received in revised form: 2025-11-23
Accepted: 2025-11-25
Available online: 2025-11-25

Keywords: *Solid-liquid equilibrium; Solid-gas equilibrium; Wax appearance temperature (WAT), Ideal activity model; Wilson activity model; Operational temperature*

ABSTRACT

The deposition of paraffinic and heavy hydrocarbons in pipelines is a major challenge in the petroleum industry during production and transportation of oil products. In this paper, the wax appearance temperature (WAT) in solid-liquid equilibria is calculated based on solid-liquid phase models for binary hydrocarbon systems under high-pressure operational conditions. These models, rooted in Won's framework for liquid-solid equilibria, employ the ideal activity coefficient to compute fugacity in the liquid phase and the Wilson activity model for the solid phase. The developed model accurately describes solid-phase equilibria in hydrocarbon systems across a wide pressure range (atmospheric to high pressures). For systems where operational temperatures exceed the critical temperature of the light component, forming solid-gas equilibria, the model assumes negligible solubility of the light component in the solid phase (zero concentration). The model predicts WAT for binary mixtures of light and heavy hydrocarbons with high precision, demonstrating an average absolute error of 1.64% and 1.19% across 13 tested systems (617 experimental data points).

Cite this article: Ghafourian, Z., Fani Kheshti, M., Saei Moghaddam, M., (2026), Determining Thermodynamic Conditions for Petroleum Wax Formation Using Activity Models in Solid-Liquid and Solid-Gas Equilibria, *Chemical Process Design*, 5(1), 54-61. http//doi.org/10.22111/cpd.2025.52907.1071

DOI: http//doi.org/10.22111/cpd.2025.52907.1071

Publisher: University of Sistan and Baluchestan.

1. Introduction

The deposition of paraffinic and heavy hydrocarbons in pipelines is a major challenge in the petroleum industry during production and transportation of oil products. When crude oil flows through pipelines, wax formation on the pipe walls reduces the pipeline's capacity. To address this issue, developing an accurate thermodynamic solid-liquid equilibrium (SLE) model for predicting petroleum deposit formation temperatures is essential. Most existing studies focus on predicting hydrocarbon deposit equilibria under reservoir conditions, while further research is needed for high-pressure environments and actual pipeline operational scenarios [1-3].

In thermodynamic modeling of solid-liquid equilibria (SLE), two-phase fugacity calculations are evaluated through:

1. γ-γ equilibrium models [4-6]
2. γ-φ equilibrium models [7-8]

For γ-γ based equilibria, both liquid and solid phase fugacities are derived from activity coefficient models. Won (1986) first applied this approach to predict solid-liquid equilibria using Regular Solution Theory for both phases [9]. Today, researchers employ various activity models for both solid and liquid phase calculations [10-11].

In γ-φ based equilibrium models, equations of state (EOS) are employed to calculate fugacity in vapor and liquid phases [12-14]. Pauly et al. [15-16] utilized the Soave-Redlich-Kwong (SRK) equation of state combined with G-Excess mixing rules to compute fugacities in both liquid and vapor phases.

Recent studies show that classical cubic equations of state, such as Peng–Robinson (PR) and Soave–Redlich–Kwong (SRK), remain widely used for predicting wax appearance temperature (WAT) in petroleum systems, Meanwhile, newer research by Shariatrad et al. (2022) used experimental data to model wax disappearance temperature (WDT) and found that accurate EOS selection strongly impacts prediction fidelity [17]. Furthermore, a recent review by Wen et al. (2025) emphasizes the limitations of traditional EOS models for wax deposition and calls for advanced or hybrid modeling approaches [18]. Also, Haoqi Chen et al. (2025) used the volumetric PR equation of state, together with the LCVM mixing law, to describe the vapor-liquid phase, while the Wilson predictive activity model accounted for the non-ideality of the solid phase by considering the pressure effect from the Poynting term. In addition, this study presented a new approach to calculate the wax disappearance temperature using the tangent plane distance (TPD). In their work, the results of the PR model in the solid phase have better results in determining the wax appearance temperature of paraffin compounds than the SRK equation of state [19].

In this paper, were proposed a new model based on solid-liquid equilibria in both phases to accurately predict two-phase solid-liquid equilibria (wax appearance temperature, WAT) in binary and multicomponent systems containing light and heavy hydrocarbons over an extended pressure range. Also, were employed activity models to predict fugacity in both liquid and solid phases. The ideal solution model is used for the liquid phase, while the Wilson predictive model [20] is applied to the solid phase. The primary objective of this proposed model is to avoid using cubic equations of state for fugacity calculations in both solid and liquid phases under both atmospheric and high-pressure conditions.

2. Thermodynamic model

The thermodynamic equilibrium of wax formation is studied using a general solid-liquid equilibrium (SLE) equation, which correlates the composition in both phases with the non-ideality of the phases and the thermophysical properties of the pure components [21]. The equilibrium ratio between the solid and liquid phases is defined as follows:

$$K_i^S = \frac{X_i^s}{X_i^l} = \frac{\phi_i^l(P,T)}{\phi_i^s(P,T)} \tag{1}$$

2.1. Solid-phase fugacity computational model

The fugacity of each component in the solid phase is calculated using the following equation:

$$f_i^S(T,P,x_1^S,...,x_N^S) = x_i^S \gamma_i^S f_{purei}^S(T,P) \tag{2}$$

The solid-phase fugacity is calculated by transforming the subcooled liquid fugacity to solid-phase fugacity at high pressure and constant temperature. Thus, Eq. (2) can be rewritten as Eq. (3):

$$f_i^S(T,P,x_1^S,...,x_N^S) = x_i^S \gamma_i^S f_{purei}^L(T,P) \times \exp\left(-\alpha_i \frac{\Delta H_{F,i}}{R^2T^2}\left(P-P^\circ\right) + \frac{\Delta H_{F,i}}{RT}\left(1-\frac{T_{F,i}}{T}\right)\right) \tag{3}$$

In Eq. (3), the parameter α_i represents the pressure-temperature slope during the solid-to-liquid phase transition, which is obtained from literature data [22]. Additionally, the parameters T_f (fusion temperature) and ΔH_f (enthalpy of fusion) correspond to the solid-to-liquid phase transition of the pure component [23]. For calculating the activity coefficients of pure components in Eq. (3), the Wilson equation is applied [20]

2.2. Liquid-phase fugacity computational model

The fugacity of each component in the liquid phase is calculated using Equation (4):

$$f_i^L(T,P,x_1^L,...,x_N^L) = x_i^L \gamma_i^L f_{pure\,i}^L(T,P) \tag{4}$$

In Eq. (4), the term γ_i^L represents the fugacity of component *i* in the liquid phase, where an ideal activity coefficient model is assumed. The term $f_{purei}^L(T,P)$ denotes the fugacity of the pure component *i* in the liquid phase. By combining Eqns. (3) and (4), we derive the following relationship to calculate the equilibrium composition of each component in the liquid and solid phases

$$x_i^L = x_i^S \gamma_i^S \times \exp\left(-\alpha_i \frac{\Delta H_{F,i}}{R^2T^2}\left(P-P^\circ\right) + \frac{\Delta H_{F,i}}{RT}\left(1-\frac{T_{F,i}}{T}\right)\right) \tag{5}$$

3. Results

In this paper, hydrocarbon binary compounds are studied in two groups: solid-liquid equilibrium between binary systems in which the ratio of the wax formation temperature to the critical temperature of one of the components is $T_r < 1$ (*i.e.*, the wax formation temperature is less than the critical temperature of the component) and binary compounds in which the ratio of the wax formation temperature to the critical temperature of the component is $T_r \geq 1$ for both components.

3.1. Binary compounds with value $T_r < 1$

In this case, 8 binary compounds were examined in which the wax formation temperature in both components was lower than the critical temperature that causes the formation of solid-liquid equilibrium, the results of which are given in Table 1. As can be seen in Table 1, these binary compounds are composed of paraffins with a high carbon number or, if they contain a light hydrocarbon component, the percentage of the light component is higher so that the wax formation temperature is lower than the critical temperature of this light component. In these cases, for most systems, the error was below 2%, and the average error in all combinations is 1.64%. This error was calculated in the calculation of the wax formation temperature at different pressures and combinations using coding in MATLAB software. Prediction of wax formation temperature in C_{14}-C_{15} mixture at three different mole percent of C_{15} (*=0.25, O=0.5 and □= 0.75) with N_2 model and its comparison with experimental results in Fig. 1 has been illustrated. In Fig. 1 until to Fig. 4, The X axis is mole fraction of heavy component and Y axis is Pressure in MPa unit.

Table 1. Error rate in calculating the wax formation temperature in binary compounds with value $T_r < 1$

Binaries	**Heavy component content range**	**Pressure range (MPa)**	**NP**	**Absolute error = sum** $\lvert T_{\exp} - T_{calc} \rvert$	**Reference**
C_{14}-C_{15}	0-1	20-100	50	1.30	[8]
C_{14}-C_{16}	0-1	20-100	70	1.88	[8]
C_6-C_{13}	0.3158-1	133-300	22	2.26	[24]
C_6-C_{16}	0.2007-0.9543	10.67-300	50	1.75	[24]
C_6-C_{18}	0.2509-0.9401	12.04-300	58	1.64	[24]
C_2-C_{16}	0.054-0.801	1.7-14.4	50	0.79	[20]
C_2-C_{20}	0.097-0.496	2.05-11.05	48	1.21	[21]
C_3-C_{34}	0.0995-0.3969	1.151-11.052	26	2.30	[22]
Average	-	-	-	1.64	-

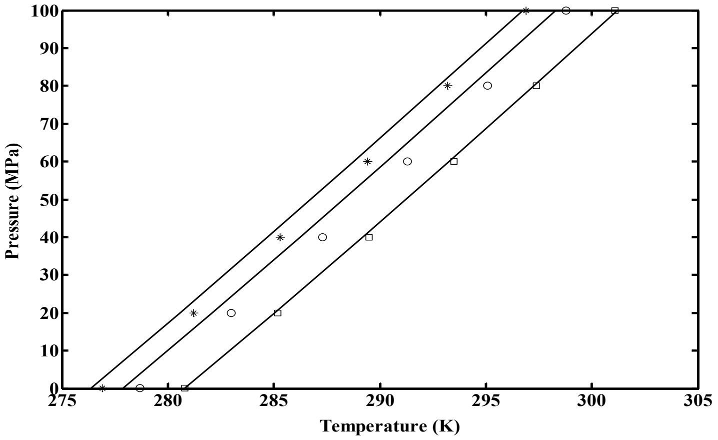

Fig. 1. Prediction of wax formation temperature in C_{14}-C_{15} mixture at three different mole percent of C_{15} (*=0.25, O=0.5 and □= 0.75) with N_2 model and its comparison with experimental results [8]

As can be seen in Fig. 2, the model's predictive ability is very good up to pressures in the 300 MPa range, and at pressures above 300 MPa, the system's diagnostic ability gradually decreases, but the average model prediction at 50 points is still 1.75, which is less than 2 degrees at very high operating pressures. In pressure Higher than 300 MPa, due to the compactness of molecules, the error of thermodynamic models in determining the parameters of molecular attraction and repulsion, as well as activity models, increases. As we know, activity models are presented for atmospheric pressures, and using them at high pressures increases the error amount. Of course, in this project we are talking about pressures of more than 3000 atmospheres.

3.2. Binary compounds with value $T_r \geq 1$

In this case, 5 binary compositions were examined in which the wax formation temperature in one of the components is lower than the critical temperature, and in other cases, the wax formation temperature is higher than the critical temperature of the light component, and in the case where the percentage of the hydrocarbon component is higher, the contribution to this binary system is greater.

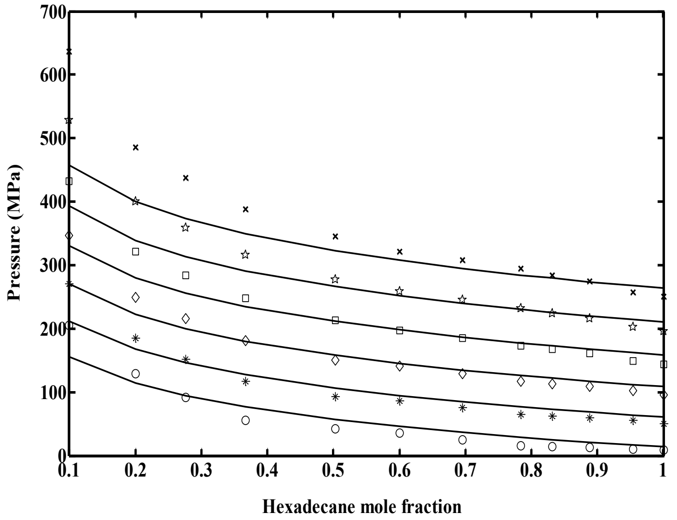

Fig. 2. Comparison of experimental values [24] and results from the N6 model in the C_6-C_{16} composition in the range of 293.15K to 343.15K. The lines of the model results and the symbols are experimental values. (O=293.15K, *= 303.15K, ◊=313.15K, □=323.15K, ☆=333.15K and ×=343.15 K)

These compounds inherently form a solid-gas equilibrium due to the lack of formation of a liquid phase, and in this case, the solubility of the light component in the solid phase is considered to be zero, and it is assumed that only the heavy component crystallizes in the solid phase and the lighter component is only present in the liquid or vapor phase, and as a result, $\gamma_i^S = 1$ and $x_i^S = 0$ are considered in the light component. As shown in Table 2, the calculation error in the samples, considering the complete crystallization of the heavy component in the solid phase, is 1.19. The average error in 5 samples is 1.19. In Fig. 3, due to the high percentage of the lighter component in the mixture, the prediction of the wax formation temperature with the assumptions considered is very accurate at all 31 points in the pressure range up to 10 MPa, and the error rate at all 31 points is 0.08 percent. Fig. 4 also shows the binary combination of methane and C17. In this combination, assuming the formation of solid-gas equilibrium and the absence of methane in the solid phase, the results were obtained with appropriate accuracy, and the error rate at 16 points is equal to 0.95, which indicates the appropriateness of the assumptions considered.

Table 2. Error rate in calculating the wax formation temperature in binary compounds with a value of $T_r \geq 1$ in one of the components

Binaries	Heavy component content range	Pressure range (MPa)	NP	Absolute error = sum $\lvert T_{\exp} - T_{calc} \rvert$	Reference
C_2+C_{20}	0.715-0.917	0.55-10.05	31	0.08	[21]
C_2+C_{22}	0.3962-0.9459	1.06-10.03	30	1.49	[23]
C_1+C_{17}	0.296-0.7979	10.01-80.08	16	0.95	[16]
C_1+C_{24}	0.256-0.901	10.11-257.5	76	2.11	[25]
C_1+C_{30}	0.103-0.85	18.1-193.1	90	1.35	[26]
Average	-	-	-	1.19	-

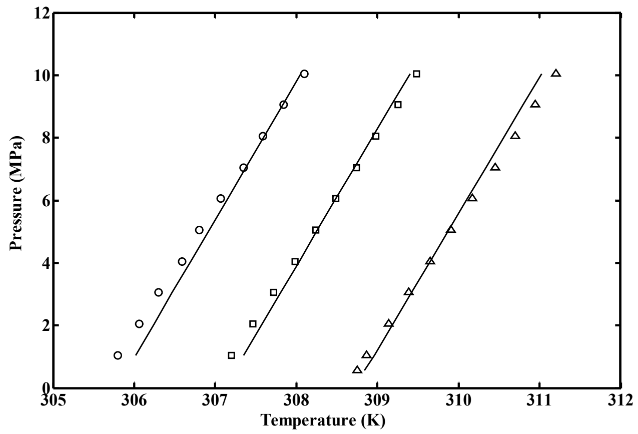

Fig. 3. Wax formation temperature in the binary C_2-C_{20} compound at high pressure and different combinations of the two materials. The values of the percentage of C_{20} in the compound are (O=0.715 □=0.801 Δ=0.917) and the lines of the calculated values

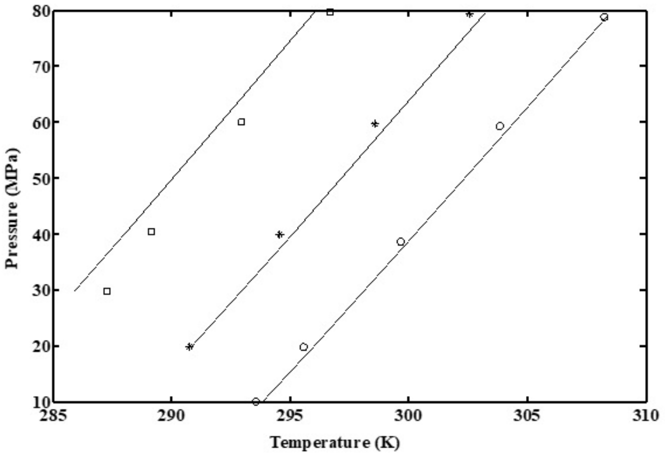

Fig. 4. Comparison of the results obtained from the wax formation conditions in the binary combination between C1-C17 and comparison with the laboratory values [16] at 3 different molar percentages of C17 (□=0.3986 *=0.6007 O=0.7979)

4. Conclusion

In this research, a new model for predicting the wax formation temperature in solid-liquid and solid-gas equilibria over a wide range of pressures close to operating pressures and compositions in binary mixtures has been studied. The activity model has been used in all liquid, solid and gas phases. In the case where the wax formation temperature is lower than the critical temperature of one of the components, The precipitation rate of that component in the solid phase is considered to be zero. Despite the assumption of no precipitation of the light component in the solid phase, the results are very accurate and demonstrate the suitability of the assumption.

One of the most important advantages of this model is its use in multi-component systems. Given that this model does not use fitted parameters and is an integrated model, it can easily be used in multi-component systems. In this model, a new approach is used to calculate the molar volume of a solid based on the calculation of the molar volume in the liquid phase. Also, new hypotheses have been investigated in the study of solid-liquid equilibria in the combination of a light hydrocarbon and a heavy hydrocarbon, which has good results, and the model introduced in this work is in good agreement with experimental data and the error rate in 13 samples was examined and in 617 laboratory data extracted from articles, it was less than 2 percent in all samples, and the average error in the samples was 1.64 and 1.19 percent.

Nomenclature

Symbols

T	Temperature (K)
P	Pressure (MPa)
γ	Activity coefficient
φ	Fugacity
Xi	Solid phase composition
Yi	Liquid (vapor) phase composition
ΔH_f	Enthalpy of fusion (j.mol^{-1})
T_f	fusion temperature (K)
P^o	Standard pressure (MPa)
R	Gas constant (m^3·Pa·K^{-1}·mol^{-1})

Abbreviation

WAT	Wax appearance temperature
SLE	Solid-liquid equilibrium
EOS	Equations of state
PR	Peng–Robinson
WDT	Wax disappearance temperature
TPD	Tangent plane distance
S	Solid phase
L	Liquid phase
V	Vapor phase

References

[1] Xue, J., Li, C., He, Q., 2019. Modeling of wax and asphaltene precipitation in crude oils using four-phase equilibrium. Fluid Phase Equilibria, 497, 122-132. https://doi.org/10.1016/j.fluid.2019.06.011

[2] Khaghani, A., Moghaddam, M.S., Kheshti, M.F., 2025. Investigation of the liquid-vapor equilibrium in the mixture of carbon dioxide and normal alkanes in binary systems using the Peng-Robinson equation of state modified with mixing rules. Chemical Thermodynamics and Thermal Analysis, 17, 100161. https://doi.org/10.1016/j.ctta.2025.100161

[3] Eniolorunda, O.V., Chapoy, A., Burgass, R., 2021. Phase equilibria of waxy live oil systems containing CO$_2$: Experimental measurements and thermodynamic modeling. Energy and Fuels, 35(5), 3731-3741. https://doi.org/10.1021/acs.energyfuels.0c02977

[4] Reddy, V.J., Ghazali, M.F., Kumarasamy, S., 2024. Advancements in phase change materials for energy-efficient building construction: A comprehensive review. Journal of Energy Storage, 81, 110494. https://doi.org/10.1016/j.est.2024.110494

[5] Tahmasbi, Y., Moghaddam, M.S., Kheshti, M.F., 2025. Prediction of the Viscosity of Saturated Liquid and Unsaturated Gaseous Chlorofluorocarbons as Well as Hydrocarbon Mixtures Using the Peng–Robinson Equation of State. Petroleum Chemistry, 65(1), 72-81. https://doi.org/10.1134/S0965544124070132

[6] Ghanaei, E., Esmaeilzadeh, F., Kaljahi, J.F., 2007. A new predictive thermodynamic model in the wax formation phenomena at high pressure condition. Fluid phase equilibria, 254(1-2), 126-137. https://doi.org/10.1016/j.fluid.2007.02.024

[7] Yao, Y., Wu, H., 2021. Macroscale modeling of solid–liquid phase change in metal foam/paraffin composite: effects of paraffin density treatment, thermal dispersion, and interstitial heat transfer. Journal of Thermal Science and Engineering Applications, 13(4), 041024. https://doi.org/10.1115/1.4049144

[8] Milhet, M., Pauly, J., Coutinho, J.A.P., Dirand, M., Daridon, J.L., 2005. Liquid–solid equilibria under high pressure of tetradecane+ pentadecane and tetradecane+ hexadecane binary systems. Fluid Phase Equilibria, 235(2), 173-181. https://doi.org/10.1016/j.fluid.2005.06.028

[9] Won, K.W., 1986. Thermodynamics for solid solution-liquid-vapor equilibria: wax phase formation from heavy hydrocarbon mixtures. Fluid Phase Equilibria, 30, 265-279. https://doi.org/10.1016/0378-3812(86)80061-9

[10] Soares, N., Matias, T., Durães, L., Simões, P.N., Costa, J.J., 2023. Thermophysical characterization of paraffin-based PCMs for low temperature thermal energy storage applications for buildings. Energy, 269, 126745. https://doi.org/10.1016/j.energy.2023.126745

[11] Schou Pedersen, K., Skovborg, P., Roenningsen, H.P., 1991. Wax precipitation from North Sea crude oils. 4. Thermodynamic modeling. Energy and Fuels, 5(6), 924-932. https://doi.org/10.1021/ef00030a022

[12] Cao, J., Liu, L., Liu, C., He, C., 2022. Phase transition mechanisms of paraffin in waxy crude oil in the absence and presence of pour point depressant. Journal of Molecular Liquids, 345, 116989. https://doi.org/10.1016/j.molliq.2021.116989

[13] Lira-Galeana, C., Firoozabadi, A., Prausnitz, J.M., 1996. Thermodynamics of wax precipitation in petroleum mixtures. AICHE journal, 42(1), 239-248. https://doi.org/10.1002/aic.690420120

[14] Ji, H.Y., Tohidi, B., Danesh, A., Todd, A.C., 2004. Wax phase equilibria: developing a thermodynamic model using a systematic approach. Fluid Phase Equilibria, 216(2), 201-217. https://doi.org/10.1016/j.fluid.2003.05.011

[15] Pauly, J., Daridon, J.L., Coutinho, J.A., Lindeloff, N., Andersen, S.I., 2000. Prediction of solid–fluid phase diagrams of light gases–heavy paraffin systems up to 200 MPa using an equation of state–GE model. Fluid Phase Equilibria, 167(2), 145-159. https://doi.org/10.1016/S0378-3812(99)00316-7

[16] Pauly, J., Coutinho, J., Daridon, J.L., 2007. High pressure phase equilibria in methane+ waxy systems: 1. Methane+ heptadecane. Fluid phase equilibria, 255(2), 193-199. https://doi.org/10.1016/j.fluid.2007.04.014

[17] Shariatrad, F., Javanmardi, J., Rasoolzadeh, A., Mohammadi, A.H., 2022. Experimental Measurement and Thermodynamic Modeling of the Wax Disappearance Temperature (WDT) for a Quaternary System of Normal Paraffins. ACS omega, 7(20), 16928-16938. https://doi.org/10.1021/acsomega.1c07072

[18] Wen, J., Lu, Y., Jia, Y., Luo, H., You, C., Huang, Z., Wang, C., Luo, Y., 2025. Progress on Wax Deposition Characteristics and Prediction Methods for Crude Oil Pipelines. Processes, 13(6), 1651. https://doi.org/10.3390/pr13061651

[19] Chen, H., Shi, B., Guo, E., Song, S., Kang, Q., Yao, H., Chen, H., Wu, H., Gong, J., 2025. A thermodynamic model with stability testing for wax precipitation in paraffin systems. Fuel, 401, 135897. https://doi.org/10.1016/j.fuel.2025.135897

[20] Wilson, G.M., 1964. Vapor-liquid equilibrium. XI. A new expression for the excess free energy of mixing. Journal of the American Chemical Society, 86(2), 127-130. https://doi.org/10.1021/ja01056a002

[21] Prausnitz, J.M., Lichtenthaler, R.N., De Azevedo, E.G., 1998. Molecular thermodynamics of fluid-phase equilibria. Pearson Education.

[22] Nasrifar, K., Moshfeghian, M., 2012. Multiphase equilibria of waxy systems with predictive equations of state and a solid solution model. Fluid phase equilibria, 314, 60-68. https://doi.org/10.1016/j.fluid.2011.10.019

[23] De Goede, R., Peters, C.J., Van Der Kooi, H.J., Lichtenthaler, R.N., 1989. Phase equilibria in binary mixtures of ethane and hexadecane. Fluid phase equilibria, 50(3), 305-314. https://doi.org/10.1016/0378-3812(89)80297-3

[24] Peters, C.J., De Roo, J.L., Lichtenthaler, R.N., 1991. Measurements and calculations of phase equilibria in binary mixtures of ethane+ eicosane: Part 3. Three-phase equilibria. Fluid phase equilibria, 69, 51-66. https://doi.org/10.1016/0378-3812(91)90025-3

[25] Peters, C.J., De Roo, J.L., de Swaan Arons, J., 1992. Measurements and calculations of phase equilibria in binary mixtures of propane+ tetratriacontane. Fluid Phase Equilibria, 72, 251-266. https://doi.org/10.1016/0378-3812(92)85029-8

[26] Peters, C.J., Spiegelaar, J., Arons, J.D.S., 1988. Phase equilibria in binary mixtures of ethane+ docosane and molar volumes of liquid docosane. Fluid Phase Equilibria, 41(3), 245-256. https://doi.org/10.1016/0378-3812(88)80009-8

[27] Domańska, U., Morawski, P., 2004. Solid+ liquid equilibria of (n-alkane+ cyclohexane) mixtures at high pressures. Fluid phase equilibria, 218(1), 57-68. https://doi.org/10.1016/j.fluid.2003.11.017

[28] Pauly, J., Coutinho, J., Daridon, J.L., 2007. High pressure phase equilibria in methane+ waxy systems: 1. Methane+ heptadecane. Fluid phase equilibria, 255(2), 193-199. https://doi.org/10.1016/j.fluid.2007.04.014

[29] Flöter, E., De Loos, T.W., de Swaan Arons, J., 1997. High pressure solid-fluid and vapour-liquid equilibria in the system (methane+ tetracosane). Fluid phase equilibria, 127(1-2), 129-146. https://doi.org/10.1016/S0378-3812(96)03157-3